TOPICAL REVIEW — High pressure physics

High-pressure studies on heavy fermion systems*

Ye Chen(陈晔), Zongfa Weng(翁宗法), Smidman Michael,
Xin Lu(路欣)†, and Huiqiu Yuan(袁辉球)‡

Center for Correlated Matter and Department of Physics, Zhejiang University, Hangzhou 310058, *China*

(Received 21 July 2015; revised manuscript received 25 August 2015; published online 1 June 2016)

In this review article, we give a brief overview of heavy fermions, which are prototype examples of strongly correlated electron systems. We introduce the application of physical pressure in heavy fermion systems to construct their pressure phase diagrams and to study the close relationship between superconductivity (SC) and other electronic instabilities, such as antiferromagnetism (AFM), ferromagnetism (FM), and valence transitions. Field-angle dependent heat capacity and point-contact spectroscopic measurements under pressure are taken as examples to illustrate their ability to investigate novel physical properties of the emergent electronic states.

Keywords: heavy fermion, high pressure, superconductivity

PACS: 62.50.–p, 74.62.Fj, 74.70.Tx **DOI:** 10.1088/1674-1056/25/7/077401

1. Introduction

When a tiny amount of magnetic impurities, e.g., Mn or Fe, are doped into a good metal, the local moments of the magnetic impurities are compensated by the opposite spins of the conduction electrons, forming a Kondo singlet.[1] As a result, the scattering rate of conduction electrons by the impurities diverges as the temperature approaches zero, giving rise to a logarithmic increase of the electrical resistivity below the Kondo temperature $T_{\rm K}$. Heavy fermion systems usually refer to certain intermetallic compounds containing lanthanide (Ce, Yb, Pr, etc.) or actinide (U, Pu, Np, etc.) elements, where the localized electrons in partially filled 4f or 5f orbits form a periodic lattice and are strongly hybridized with the conduction electrons via the Kondo effect. Upon reducing the temperature of such a Kondo lattice system, the electrical resistivity $\rho(T)$ typically shows an initial increase due to the scattering by 4f or 5f localized electrons acting as Kondo impurities, reaching a maximum at a certain temperature before decreasing rapidly with further cooling. This characteristic temperature is commonly called the coherence temperature, below which Kondo scattering becomes coherent and the system gradually evolves into a new quantum state that shows Landau–Fermi liquid behavior. However, the renormalized electron mass is much heavier than that of free electrons due to the hybridization between localized electrons and conduction electrons, yielding an anomalous enhancement of the electronic specific heat coefficient γ. The term "heavy fermion" has thus been coined to distinguish the behavior of this class of materials from that of a normal Fermi liquid in metals.[2]

Besides the Kondo interaction, there exists another competing interaction in heavy fermion systems, the Ruderman–Kittel–Kasuya–Yosida (RKKY) interaction.[3–5] The Kondo interaction screens the magnetic moments of localized f electrons, leading to the formation of a heavy fermion Fermi-liquid state. On the other hand, the RKKY interaction favors long-range magnetic order, where the localized electrons can polarize the surrounding conduction electrons to form a spin density wave in space, aligning the spins of other distant f electrons. The temperatures characterizing the Kondo interaction ($T_{\rm K}$) and the RKKY interaction ($T_{\rm RKKY}$) can both be expressed in terms of the hybridization constant J between the localized and conduction electrons and the density of states at the Fermi energy $D(\varepsilon_{\rm F})$, but they follow different behaviors. The Kondo temperature is characterized by

$$T_{\rm K} \propto \exp\left(-\frac{1}{JD(\varepsilon_{\rm F})}\right), \tag{1}$$

and the RKKY temperature can be written as

$$T_{\rm RKKY} \propto D(\varepsilon_{\rm F})J^2. \tag{2}$$

The competition between the Kondo and RKKY interactions in heavy fermion systems may result in various ground states, leading to a rich phase diagram, which can be qualitatively described by the Doniach phase diagram as schematically shown in Fig. 1.[6] The hybridization constant J can be effectively tuned by pressure, chemical doping, or magnetic field because the associated energy scales are relatively small in heavy fermion compounds. When J is small, the RKKY interaction

*Project supported by the National Basic Research Program of China (Grant No. 2011CBA00103), the National Natural Science Foundation of China (Grant Nos. 11174245 and 11374257), the Science Challenge Program of China, and the Fundamental Research Funds for the Central Universities of China.

†Corresponding author. E-mail: xinluphy@zju.edu.cn

‡Corresponding author. E-mail: hqyuan@zju.edu.cn

© 2016 Chinese Physical Society and IOP Publishing Ltd

becomes dominant and the system exhibits a magnetic ground state, e.g., antiferromagnetic order. With increasing hybridization, the Kondo interaction is enhanced and the system may exhibit heavy fermion behavior. At a critical value J_c, the system may experience a continuous phase transition at zero temperature, i.e., a quantum critical point (QCP), changing the ground state from a magnetically ordered state to a disordered state, which is driven by quantum fluctuations instead of thermal fluctuations. Near the quantum critical point of heavy fermion compounds, exotic quantum states and anomalous normal-state behavior have been widely observed. For example, the specific heat C/T diverges logarithmically and the resistivity shows linear rather than quadratic temperature dependence as the temperature approaches zero. The universality of the critical behaviors and its underlying mechanism remains unresolved. On the other hand, the discovery of superconductivity in the heavy fermion compound $CeCu_2Si_2$ with $T_c \simeq 0.6$ K by Frank Steglich in 1979 challenged the conventional BCS theory and pioneered research into unconventional superconductivity.[7] Until now, more than 40 heavy fermion superconductors have been discovered. The interplay of superconductivity and magnetism as well as its relationship to quantum criticality remains an important but open issue in heavy fermion systems. The elucidations of these properties and the underlying mechanisms may shed light on the puzzles of high-temperature superconductivity.

Among various tuning parameters, physical pressure serves as a powerful tool to study the physics of heavy fermion systems because it is a clean and effective method to tune the electron interactions without breaking time reversal symmetry. In this review article, we illustrate the wide applicability of physical pressure for exploring emergent quantum states, in particular superconductivity and quantum criticality in heavy fermion systems.

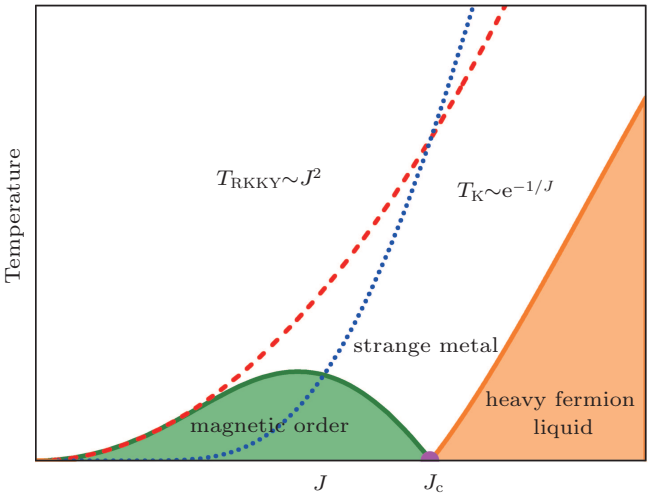


Fig. 1. (color online) A schematic illustration of the Doniach phase diagram.

2. Experimental techniques under pressure

Measurements of transport properties under pressure have been widely employed to study emergent phenomena in correlated electron systems and are powerful tools for determining the presence of pressure-induced phase transitions, metal–insulator transitions and anomalous normal-state behavior. In order to reveal the pressure-induced superconducting pairing states, the scaling behaviors near a pressure-induced QCP or other unusual electronic states, it is essential to extend the measurements of thermodynamic and magnetic properties to the multiple extreme conditions of low temperatures, high pressure and high magnetic field. In this section, we describe a few experimental methods which were recently set up in our laboratory and are very useful for studying the order parameters of pressure-induced phase transitions. They are the ac calorimetry and the point-contact spectroscopy under the aforementioned multiple extreme conditions, while the former method can be even measured in a pressure cell with a rotating magnetic field down to mK temperatures.

AC calorimetry is an alternative option for specific heat measurements under pressure,[8] since the commonly used relaxation method cannot be performed in the pressure environment. The disadvantage of not being able to determine the absolute value from ac calorimetry is compensated by its high resolution and valuable information about thermodynamic properties can be obtained from measurements of bulk phase transitions. Figure 2(a) is a schematic drawing of the ac calorimetry technique. The heater and thermometer are both thermally connected to the sample, which is anchored to a thermal bath at a temperature T_0 through a thermal link κ_1. In principle, the sample itself should have a good thermal link to the heater and thermometer, which can be defined as κ_2. If the ac current to the heater has a frequency of $\omega/4\pi$, i.e., $I = I_0\cos(\omega t/2)$, the heating power to the sample is $P = P_0[1+\cos\omega t]$, generating an ac temperature oscillation $T_{ac}\cos\omega t$, with a frequency $\omega/2\pi$. By solving the one-dimensional heat flow equation, Sullivan and Seidel obtained the following relationship between the temperature oscillation amplitude T_{ac} and the sample heat capacity C:[8,9]

$$T_{ac} = \frac{P_0}{2\omega C}\left[1+\frac{1}{\omega^2\tau_1{}^2}+\omega^2\tau_2^2\right]^{-0.5}, \tag{3}$$

where $\tau_1 = C/\kappa_1$ and $\tau_2 = C/\kappa_2$ are the corresponding thermal relaxation time and $\tau_1 \gg \tau_2$ usually holds. From this equation, it is obvious that T_{ac} generally has a frequency dependence. In the low-frequency region, i.e., $\omega \ll 1/\tau_1$, $T_{ac} = P_0/\kappa$ is a constant and is independent of the sample specific heat. In the high-frequency region $\omega \gg 1/\tau_2$, T_{ac} is almost zero and the heat power acts only to maintain the sample at a constant temperature. Therefore, an optimal frequency region should be chosen, where $1/\tau_1 \ll \omega \ll 1/\tau_2$ and the original equation

can be simplified to $T_{ac} = P_0/2\omega C$, which is determined only by the heat power and its frequency.

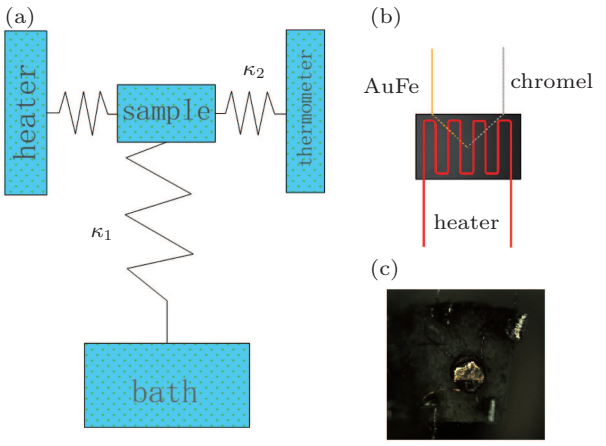


Fig. 2. (color online) (a) Schematic thermodynamic model of ac calorimetry measurements. (b) Diagram of sample preparation for the ac calorimeter. (c) Photograph of the ac calorimetric setup inside a piston cylinder pressure cell.

The experimental setup of the ac calorimetry measurements is shown in Fig. 2(b). The heater consists of constantan wire in a zigzag shape and GE Vanish is used to make good thermal contact with the sample. The ac temperature oscillation is detected by an AuFe–NiCr thermocouple and the small ac voltage signal is detected using a lock-in amplifier with a low noise transformer. Figure 2(c) shows the photograph of a sample on the plug of a piston-cylinder pressure cell prepared for ac calorimetry measurements.

Restricted by the pressure cells, some advanced experimental methods, such as the angle-resolved photoemission spectroscopy (ARPES), are not able to characterize the pressure-induced superconductivity. Field-angle dependence of the heat capacity is a useful tool for detecting nodal positions in the superconducting gap and thus allows us to determine the superconducting order parameters, serving as an invaluable alternative for probing unconventional superconductivity emerging under pressure, thanks to the ability of measuring the heat capacity under pressure using ac calorimetry. However, it is difficult to adapt a pressure cell to a commonly used mechanical rotator in a cryostat. Thus, a vector magnet, which can generate a magnetic field along any direction, is usually required for such measurements.

The relevant theory for the field-angle dependence of gap symmetries was proposed by Vekhter *et al.* by analyzing the Doppler energy shift caused by a supercurrent flowing around a vortex in a magnetic field,[10] given by $\delta E = \boldsymbol{v}_s \hbar \boldsymbol{k}_F$, where $\boldsymbol{v}_s$ represents the velocity of the supercurrent and $\hbar \boldsymbol{k}_F$ is the Fermi momentum of the nodal quasiparticles. In the case of unconventional superconductivity with gap nodes, the Doppler energy shift plays an important role in breaking Cooper pairs around the nodal positions and thus mainly contributes to the low-energy extended quasiparticle excitations at low temperatures, when the applied magnetic field is far below the upper critical field ($B \ll B_{c2}$) and a vortex lattice is induced.[11] Taking a d-wave superconductor with line nodes as an example, the in-plane field-angle dependence of the specific heat displays four-fold symmetry. When the magnetic field is along a nodal direction, the two nodal positions perpendicular to the applied field contribute to the electronic density of states ρ_0, while the other two do not. On the other hand, when the magnetic field is along an antinodal direction, the four nodal positions make equal contributions to $\rho_0/\sqrt{2}$. If a magnetic field is rotated in the *ab* plane, a four-fold oscillation of the density of states can be observed either in specific heat or thermal conductivity measurements at a finite temperature far below T_c, where the minima correspond to the gap node directions. In reality, the identification of the nodal positions may be complicated by quasiparticle scattering in the vortex lattice and the amplitude of the oscillations is generally reduced to a few percent of the background value.

Field-angle dependent heat capacity measurements have been applied to detect the gap symmetries of the widely studied Ce-based "115" heavy fermion systems such as $CeCoIn_5$, $CeIrIn_5$, and $CeRhIn_5$ under pressure,[12–15] which are generally believed to be d-wave superconductors with a $d_{x^2-y^2}$ order parameter. An oscillation sign reversal was observed in the in-plane field-angle dependent specific heat measurements of $CeCoIn_5$ when cooled below 200 mK, which is about $0.1T_c$. The evolution of the oscillation amplitude with temperature and applied magnetic field is consistent with the calculations of a $d_{x^2-y^2}$ gap structure.[12] In the case of $CeIrIn_5$, there is a long-standing debate about whether the superconductivity originates from spin or valence fluctuations.[16–18] At ambient pressure $CeIrIn_5$ lies near the cusp of two superconducting domes, as shown in Fig. 3(a),[19,20] and its bulk T_c increases to 1.0 K under pressure, even further away from the region with strong antiferromagnetic fluctuations. However, the field-angle dependence of the specific heat of $CeIrIn_5$ under pressure, as shown in Fig. 3(b), is still consistent with a $d_{x^2-y^2}$ gap symmetry up to 2.05 GPa.[21] Moreover, an oscillation sign reversal is observed at 0.9 GPa, as shown in Fig. 3(c),[21] where the heat capacity minima switch from the antinodal to nodal directions, in agreement with the theoretical predictions proposed by Vekhter *et al.* in 2008.[22] These results suggest a $d_{x^2-y^2}$ gap symmetry for the "115" heavy fermion systems which will be further discussed later.

The point-contact spectroscopy (PCS) serves as another important tool for investigating the electronic states and superconducting gap symmetries at ambient or pressure conditions, which is complimentary to the scanning tunneling microscope (STM) technique. While mechanical PCS techniques require a tiny metal needle to make point-like contact with the sam-

ple, the soft point contact is simply made by thin platinum wire glued to the sample using silver paint or silver epoxy, as shown in Figs. 4(a) and 4(b), respectively. The setup is prepared in a similar manner as for resistivity measurements and, therefore, it can also be applied under pressure. With the advantages of being easy to adapt to a pressure environment, soft point-contact spectroscopy becomes a unique tool for exploring the exotic electronic states emerging under pressure, while other experimental methods, such as STM or ARPES, can only be performed in a high vacuum environment.

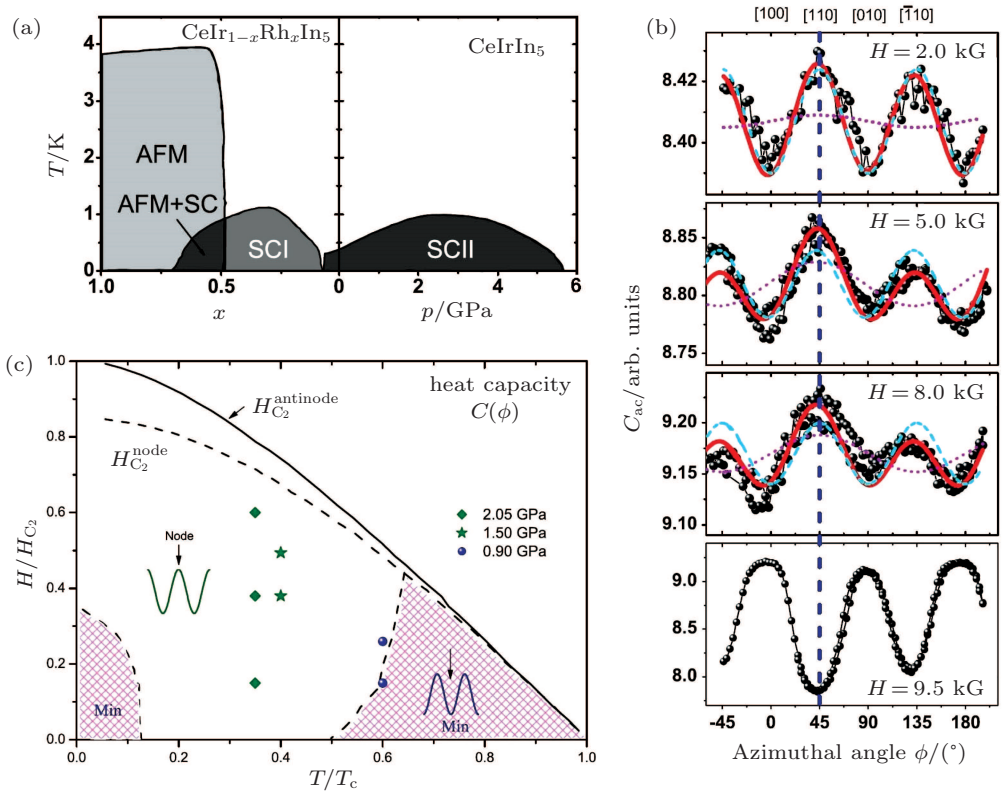


Fig. 3. (color online) (a) Two superconducting domes in Rh-doped $CeIrIn_5$ and $CeIrIn_5$ under pressure. (b) Field-angle dependence of the ac specific heat in different magnetic fields for $CeIrIn_5$, where $p = 2.05$ GPa and $T = 0.3$ K. (c) Theoretical B–T phase diagram for the four-fold field-angle dependence of the specific heat, together with the experimental data of $CeIrIn_5$ (adapted from Ref. [21]).

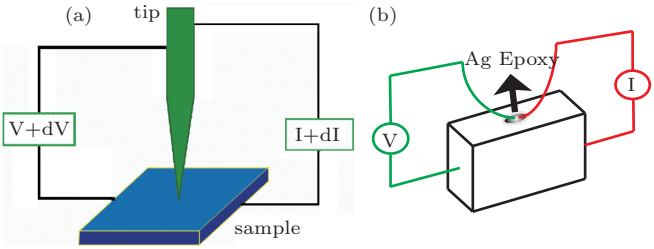


Fig. 4. (color online) Sketch for (a) mechanical and (b) soft point-contact spectroscopy.

Both mechanical and soft point-contact spectroscopic methods are commonly applied to investigate the superconducting gap and order parameter symmetries in various superconductors such as MgB_2 and iron-based superconductors.[23] In general, Andreev reflection is associated with the transmission across the interface in the presence of a partial tunneling barrier, where an electron is retroreflected as a hole and one Cooper pair goes through the interface with the conductance doubled inside the superconducting gap.[24] The experimental conductance curves $G(V)$ are analyzed with the Blonder–Tinkham–Klapwijk (BTK) model to infer the gap structure or order parameter symmetries,[25] which will not be extensively discussed here and can be referenced in textbooks or review articles.[23,26] In recent years, PCS has also been extended to study the hybridization between localized f electrons and conduction electrons in heavy fermion systems, where asymmetric Fano-line shape or hybridization gap is observed due to the quantum interference between the local f and itinerant conduction electrons.[27–30] PCS has become an effective method to study the systematical evolution of the hybridization in heavy fermion systems tuned by pressure as another dimension.

As an example, here we apply the PCS technique to study the electronic structure of the pressurized URu_2Si_2. Upon cooling down, URu_2Si_2 shows two subsequent phase transitions; one is a second-order transition at $T_0 \sim 17.5$ K associated with the "hidden order" and the other is a superconducting transition with $T_{sc} \sim 1.5$ K.[31] The nature of the "hidden order" has received intensive attention in recent years but remains a mystery.[32] The application of pressure suppresses

superconductivity around 0.5 GPa but slightly enhances T_0.[33] With further increasing pressure, a large-moment antiferromagnetic (LMAF) phase emerges from the hidden order phase via a first-order-like transition and its transition temperature $T_{\rm LMAF}$ continues to increase, merging with T_0 at a critical pressure of around 1.3 GPa. The LMAF phase directly emerges from the high-temperature paramagnetic state at higher pressures. In Fig. 5, we plot the soft point-contact spectroscopy of URu_2Si_2 at ambient pressure and 1.62 GPa, which allows us to look into the evolution of electronic properties in the "hidden order" state and the LMAF state.[34] It is found that two asymmetric peaks emerge below the ordering temperature at both $p = 0$ and $p = 1.62$ GPa. The charge gaps which are characterized by the distance between the two asymmetric peaks, are similar in both states with only a tiny increase with pressure, indicating the robustness and probably common origin of the charge gap between the hidden order and the LMAF state.

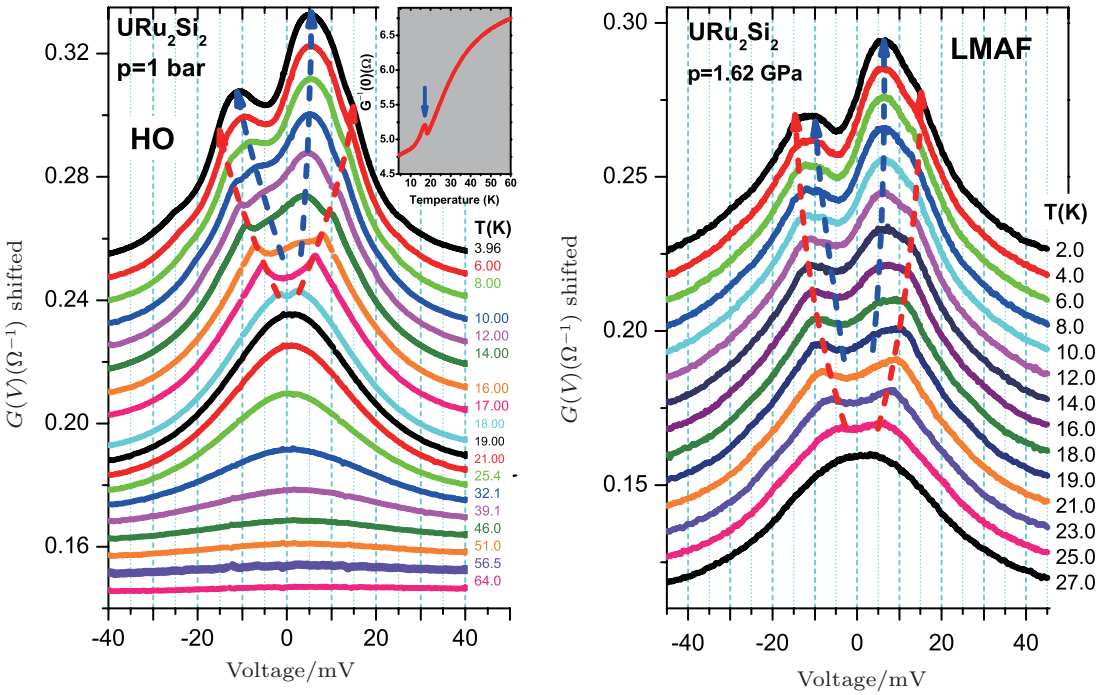


Fig. 5. (color online) Point contact spectroscopy of URu_2Si_2 at ambient pressure and 1.62 GPa (adapted from Ref. [34]).

3. Pressure-induced superconductivity

3.1. Superconductivity near an antiferromagnetic instability

A common thread in unconventional superconductors, such as heavy fermions, high-T_c cuprates or the newly discovered iron-based superconductors, is that superconductivity occurs in proximity to antiferromagnetism upon tuning non-thermal parameters, indicating a close relationship between AFM and SC. In high-T_c cuprates or iron-based superconductors, antiferromagnetism in the parent compound is generally suppressed by electron or hole doping, while both pressure and doping can tune heavy fermion systems between AFM and SC states because of their low-energy scales and thus sensitivity to changes in external parameters. For example, a superconducting dome was observed in $CePd_2Si_2$ and $CeIn_3$ under pressure with a maximum T_c near the antiferromagnetic QCP, and the origin of superconductivity was attributed to spin fluctuations.[35] Subsequently, similar phase diagrams have been observed in a number of heavy fermion compounds, in particular Ce-based compounds, e.g., $CeCu_2Si_2$,[36] CeMIn$_5$ (M = Co, Rh, Ir),[37–39] and CeMSi$_3$.[40,41] In this section, we will take the prototype compounds CeMIn$_5$ as examples and describe the intimate relationship between antiferromagnetism, quantum criticality, and superconductivity.

$CeCoIn_5$ has the highest superconducting transition temperature among the Ce-based heavy fermion systems with $T_c \sim$ 2.3 K at ambient pressure[37] and its maximum T_c reaches 2.6 K at around 1.5 GPa.[42] It is generally believed that $CeCoIn_5$ is in close proximity to an antiferromagnetic quantum critical point, where its normal state resistivity shows a linear temperature dependence[43] and the specific heat coefficient diverges logarithmically when the applied magnetic field approaches the upper critical field $B_{c2}(0)$.[37] In addition, the nuclear spin relaxation rate shows critical behavior with a $T^{1/4}$ dependence as a function of temperature.[44]

Figure 6(a) shows the pressure–temperature phase diagram of $CeRhIn_5$,[45,46] which is an antiferromagnet with a Néel transition at $T_N \simeq 3.8$ K. Upon applying pressure, T_N

initially increases and then is gradually suppressed, coexisting with the emergent bulk superconductivity first observed at 1.15 GPa ($T_c \sim 0.36$ K). The AFM in $CeRhIn_5$ suddenly collapses and exhibits a first-order-like transition when T_N is equal to T_c at $p_1 = 1.75$ GPa, driving the system from a state where AFM and SC coexist, to a pure superconducting state.[45,46] Below p_1, the superconducting transition temperature, determined from the resistivity (T_c^{ρ}) and the specific heat ($T_c^{C_p}$), shows a discrepancy, which may be attributed to the emergence of textured superconductivity associated with a switch of the magnetic structure as indicated by neutron scattering measurements.[47] The superconducting T_c is maximized at 2.3 K at $p_2 \simeq 2.3$ GPa and vanishes at about 3.8 GPa. The system displays a broad superconducting dome before entering a heavy-Fermi-liquid state at higher pressures. In the pressure range from 1.75 to 2.35 GPa, long-range antiferromagnetic order is recovered in the superconducting state when a sufficient magnetic field is applied in the ab plane, which terminates at the extrapolated antiferromagnetic QCP at around 2.35 GPa.[14,45,46] This field-induced magnetism may be attributed to the formation of an antiferromagnetic ground state in the normal regions of the vortex cores in an applied magnetic field, which requires further detailed studies.

Evidence for the existence of non-Fermi liquid (NFL) behavior and antiferromagnetic quantum criticality was shown in $CeRhIn_5$ at around 2.35 GPa, coinciding with the maximum superconducting transition temperature of $T_c \sim 2.3$ K, from a careful analysis of the specific heat and resistivity under pressure.[45,46] Its resistivity follows a sub-linear temperature dependence ($\rho \propto T^{0.85}$) in the normal state, which survives down to at least 250 mK, when superconductivity is completely destroyed by a magnetic field of 10 T.[48] The specific heat diverges when superconductivity is suppressed by applying a magnetic field,[45,46] also indicating non-Fermi liquid behavior. In the contour color plot of the isothermal resistivity shown in Fig. 6(b),[48] the maximum residual resistivity is centered around the critical pressure where T_c is also a maximum, suggesting enhanced quasiparticle scattering around the QCP and a close relationship between quantum criticality and unconventional superconductivity. Moreover, the sub-linear temperature dependence of the resistivity contradicts the theoretical predictions concerning magnetic instabilities, where the exponent should be 1.0 (1.5) for two-dimensional (three-dimensional) magnetic fluctuations. A de Haas–van Alphen effect (dHvA) study under pressure by Shishido *et al.*[49] demonstrates that the frequency branches and thus the Fermi surface exhibit a sharp change crossing the QCP at around 2.3 GPa, signalling the delocalization of Ce 4f electrons into the Fermi surface, consistent with the scenario of local quantum criticality due to Kondo breakdown across the QCP,[50,51] rather than the conventional SDW scenario.[52–54]

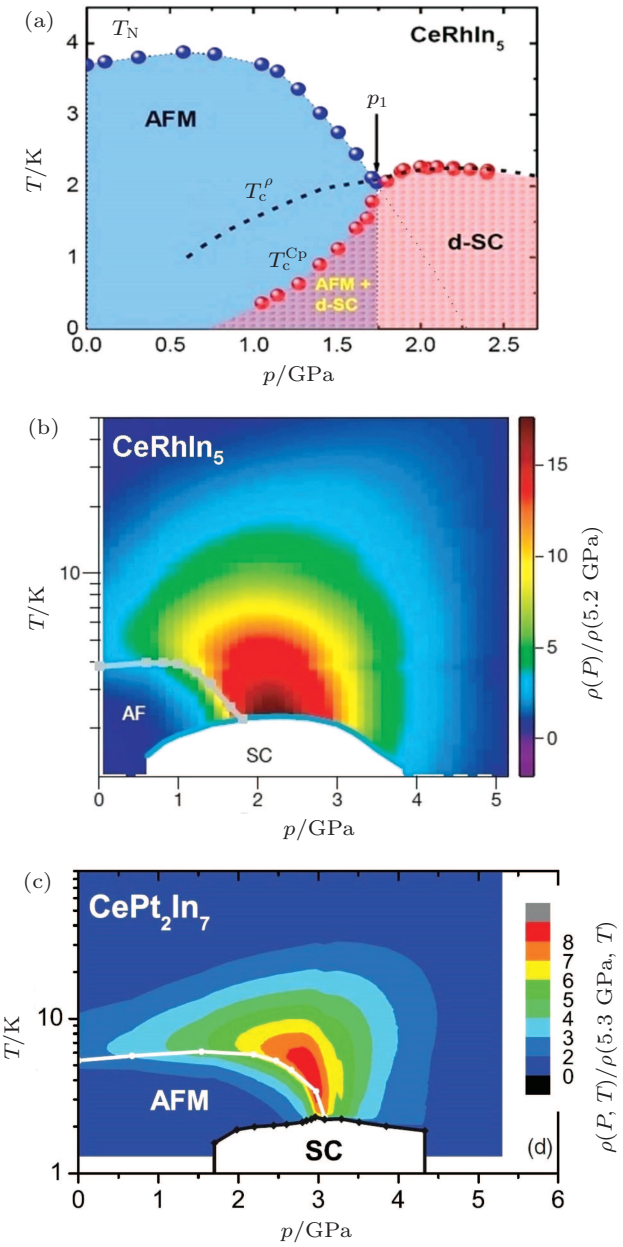


Fig. 6. (color online) (a) Pressure–temperature phase diagram of $CeRhIn_5$, where the blue symbols represent the Néel temperature T_N and the red represents the bulk superconducting transition temperature $T_c^{C_p}$, which merges with the dashed line representing the resistive superconducting transition temperature (T_c^{ρ}) at $p_1 = 1.75$ GPa (adapted from Ref. [45]). (b) Contour color plot for the normalized residual resistivity of $CeRhIn_5$ as a function of temperature and pressure (adapted from Ref. [48]). (c) Contour color plot for the normalized residual resistivity of $CePt_2In_7$ as a function of temperature and pressure (adapted from Ref. [55]).

Similar behaviors have also been observed in other heavy fermion materials with quantum criticality such as $CePt_2In_7$,[55] as shown in Fig. 6(c). The Néel temperature of $CePt_2In_7$ first slightly increases and then decreases with increasing pressure, before being suppressed to zero temperature at 3.2 GPa. Around the critical point, superconductivity emerges and a maximum of the residual resistivity and NFL behavior are found to correspond with the maximum in T_c of 2.3 K. The properties of $CePt_2In_7$ suggest that the phenomena observed close to the antiferromagnetic QCP in $CeRhIn_5$

should be commonly found.

At ambient pressure, $CeIrIn_5$ is superconducting with a bulk T_c of 0.4 K, but has a resistive transition at $T_c \simeq 1.2$ K.[56] Its superconducting transition temperature reaches a maximum value of $T_c = 1.05$ K at around 2 GPa in resistivity data.[57] A small amount of Cd doping into the In site suppresses superconductivity and induces long-range antiferromagnetic order in $CeIrIn_5$.[58] Moreover, the doped system can be tuned back to bulk superconductivity by applying pressure, as shown in Fig. 7(a).[59] The ac calorimetry data show that the Néel temperature of the 1% Cd doped $CeIrIn_5$ initially increases with pressure, reaching a maximum value of 3.1 K at around 1.3 GPa. Further increasing pressure suppresses the antiferromagnetic order and bulk superconductivity suddenly appears at 2.5 GPa with $T_c \sim 0.8$ K. The re-emergence of superconductivity indicates the reversibility between Cd doping and physical pressure, but further analysis of resistivity data poses some problems, as shown in Fig. 7(b). As pressure suppresses the antiferromagnetic state, the residual resistivity also decreases, which is the opposite case to $CeRhIn_5$[48] and $CePt_2In_7$,[55] indicating the absence of quantum criticality. The results suggest the local nature of the Cd dopant in forming long-range antiferromagnetic order, which may be due to spin fluctuations.[59] Evidence of $CeIrIn_5$ being in the vicinity of an antiferromagnetic QCP also comes from the doping studies.[60] The substitution of Hg at the In site suppresses superconductivity and drives the system to an antiferromagnetic ground state, while Sn substitution at the In site or Pt at the Ir site drives the system towards a Fermi liquid ground state. The critical concentration is at $x_{Hg} = 0.027$ in $CeIrIn_{5-x}Hg_x$, where NFL behavior is observed in a wide temperature region. These facts strongly suggest that superconductivity in $CeIrIn_5$ originates from spin fluctuations rather than valence fluctuations as previously proposed in Refs. [17] and [18].

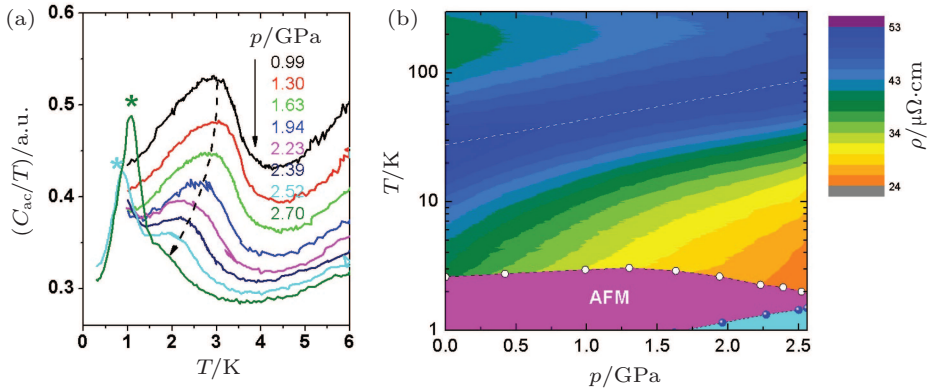


Fig. 7. (color online) (a) Pressure evolution of the heat capacity of the 1% Cd doped $CeIrIn_5$. (b) Contour color plot of the resistivity of 1% Cd doped $CeIrIn_5$ as a function of temperature and pressure (adapted from Ref. [59]).

3.2. Ferromagnetism and superconductivity

Ferromagnetism is generally believed to be antagonistic to superconductivity and their interplay in heavy fermion systems has thus been much less frequently studied. However, the coexistence of FM and SC has been observed in some actinide compounds with 5f electrons, such as URhGe,[61] UCoGe,[62] UGe_2,[63] and UIr,[64] where exotic superconducting states and rich physical phenomena are observed. Furthermore, a field-induced re-entrance of superconductivity was observed at $B \geq 8$ T in the ferromagnetic superconductor URhGe,[61] where superconductivity is initially destroyed by a field of about 2 T. The non-centrosymmetric ferromagnetic compound UIr undergoes three ferromagnetic phase transitions under pressure, before displaying superconductivity at the border of the third ferromagnetic phase at about 2.6 GPa.[64]

As a salient example of ferromagnetic superconductors, the U-based heavy fermion compound UGe_2 shows a Curie temperature of $T_C = 52$ K at ambient pressure, with an ordered moment of $\mu_s = 1.48\mu_B$/U, which is strictly aligned along the a axis.[65] Measurements of quantum oscillations suggest the delocalization of uranium 5f electrons which make the dominant contributions to the Fermi surface.[66] The itinerant nature of ferromagnetism in UGe_2 is also consistent with the specific heat and low-lying magnetic excitation spectra data.[68] The FM transition is gradually suppressed by applying pressure up to $p_c \simeq 15$ kbar, followed by an abrupt collapse at a first-order-like transition.[63] Superconductivity emerges in the pressure range from 9 kbar to 16 kbar with a maximum superconducting transition temperature of $T_c \sim 0.7$ K at around 12 kbar.[63] A second magnetic transition is observed below T_C (denoted as T_x), which is manifested in the derivative of the resistivity as a broad peak at 25 K,[67] as well as in specific heat,[68] Hall effect,[69] thermal conductivity,[70] and photoemission measurements.[71] Figure 8 shows the detailed pressure–temperature phase diagram of UGe_2,[72] where the transition from FM1 to FM2 is of first order but its origin

is still unresolved.[73,74] T_x is also suppressed monotonically by pressure and vanishes at p_x of around 12 kbar where the superconducting T_c reaches its maximum, leading to speculation that superconductivity may be attributed to ferromagnetic fluctuations from the FM2 QCP. As a result, a spin-triplet pairing state is proposed for UGe_2 and other ferromagnetic superconductors.[63,68] Furthermore, measurements of dHvA oscillations provide evidence for a reconstruction of the Fermi surface at a tricritical point,[66] which extends to a critical end point at $p \sim 35$ kbar and $B \sim 18$ T.

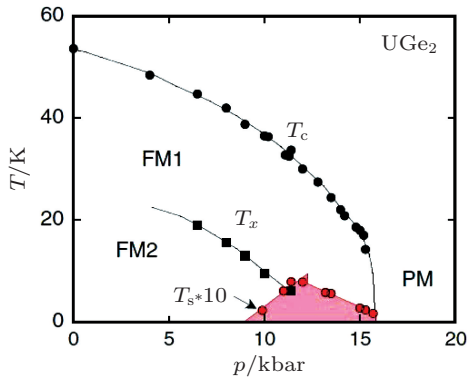


Fig. 8. (color online) The pressure–temperature phase diagram of UGe_2 (adapted from Ref. [72]).

3.3. Superconductivity near a valence instability

$CeCu_2Si_2$ is a prototype heavy fermion superconductor which lies in the vicinity of a 3D SDW quantum critical point at ambient pressure.[75] Thus, its superconductivity is generally believed to be induced by spin fluctuations. However, the pressure–temperature phase diagram of pristine $CeCu_2Si_2$ has been a puzzle in the community for a long time, since its T_c is nearly independent of pressure below 2 GPa, sharply increases to 2.3 K in the range of 2–3 GPa, followed by a slow decrease up to at least 8 GPa.[76] This step-like evolution of T_c with pressure naturally leads to the speculation that the high-pressure SC may not be attributed to a magnetic origin, but another superconducting mechanism dominates the high pressure region, since the system has a higher T_c despite being further away from the antiferromagnetic QCP.

To solve this problem, measurements of the electrical resistivity under pressure were performed for a series of Ge-doped $CeCu_2Si_2$.[77,78] Here the isoelectronic substitutions of Ge for Si in $CeCu_2Si_2$ act as a negative chemical pressure to increase the unit-cell volume. Application of pressure to $CeCu_2(Si_{1-x}Ge_x)_2$ tunes the system back to the magnetic QCP but with enhanced disorder/impurity scattering. The disorder introduced by the Si/Ge substitutions has little effect on the magnetic order, but dramatically suppresses superconductivity.[79] In Fig. 9, we plot the pressure–temperature phase diagram of $CeCu_2(Si_{1-x}Ge_x)_2$ for different Ge concentrations.[77] The pressure on the x axis is shifted by the corresponding critical pressure $p_{c1}(x)$ of each Ge concentration. One can see that the T_N line overlaps very well after the pressure shift, but superconductivity is weakened by the partial Si/Ge substitution. For x =0.1, two separate superconducting domes are observed, in contrast to a continuous superconducting dome for pure $CeCu_2Si_2$ or $CeCu_2Ge_2$. This suggests that two distinct superconducting states exist in these compounds.[77] Superconductivity in the low-pressure regime is near an antiferromagnetic instability with a maximum T_c around the QCP, which is similar to other Ce-based heavy fermion superconductors as described above, suggesting a universal scenario of magnetically mediated superconductivity in heavy fermion compounds. It should be noted that the recent measurements of specific heat at low temperatures indicate fully-gapped superconductivity in $CeCu_2Si_2$,[80] which needs to be confirmed by further experiments. T_c in the high-pressure regime reaches a much higher value and the upper critical field $B_{c2}(T)$ shows distinct scaling behavior in the two superconducting regimes,[81] suggesting a different origin of superconductivity at high pressures. Analysis of the normal-state properties suggests the existence of a second critical point in the high pressure regime.[78] Around the second critical pressure (e.g., $p_{c2} = 5.4$ GPa for 10% Ge), where T_c reaches a maximum value, the electrical resistivity $\rho(T)$ shows a linear temperature dependence but with an enhanced residual resistivity ρ_0 and a sharp drop of the resistivity coefficient A (fitted with $\rho = \rho_0 + AT^n$).[78] In addition, the specific heat measurements show an enhancement of the Sommerfeld coefficient which peaks around the critical pressure and decreases rapidly at higher pressures.[82]

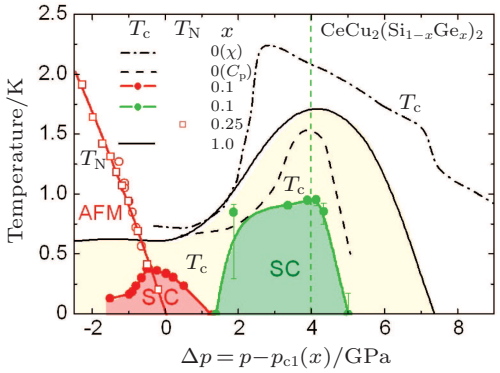


Fig. 9. (color online) The pressure–temperature phase diagram of $CeCu_2(Si_{1-x}Ge_x)_2$. The pressure on the x axis is shifted by the corresponding critical pressure $p_{c1}(x)$ at the antiferromagnetic QCP. Two superconducting states merge together in $CeCu_2Si_2$ under pressure (adapted from Ref. [77]).

These experimental features observed in the high-pressure regime of $CeCu_2(Si_{1-x}Ge_x)_2$ can be described in terms of a valence-fluctuation model,[82,83] which is based on the following generalized periodical Anderson model:

$$H = \sum_{k\sigma}(\varepsilon_k - \mu)c^{\dagger}_{k\sigma}c_{k\sigma} + \varepsilon_f \sum_{k\sigma} f^{\dagger}_{k\sigma}f_{k\sigma}$$

$$+V\sum_{k\sigma}(c^{\dagger}_{k\sigma}f_{k\sigma}+\text{h.c.})$$
$$+U_{\text{ff}}\sum_{i}n^{\text{f}}_{i\uparrow}n^{\text{f}}_{i\downarrow}+U_{\text{fc}}\sum_{i\sigma\sigma'}n^{\text{f}}_{i\sigma}n^{\text{c}}_{i\sigma'}, \quad (4)$$

where U_{fc} is an additional term describing the local Coulomb repulsion between localized f-electrons and conduction electrons. In the mean-field approximation with the slave-boson formalism, it was shown that as the f-level ε_{f} is increased relative to the Fermi level, a sharp valence change may take place by lifting the U_{fc} to the order of the band width of the conduction band. As a result, a d-wave superconducting pairing state can be stabilized by the valence fluctuations. Furthermore, this model also predicts a linear temperature dependence of the electrical resistivity, an enhancement of the residual resistivity and the specific heat coefficient γ, and a drop of the resistivity coefficient A at the valence transition, which are compatible with the experimental observations stated previously. These results suggest that superconductivity in the high-pressure regime of $CeCu_2Si_2$ is mediated by critical valence fluctuations, the first candidate compound for this new pairing mechanism.[77]

Similar ideas of two superconducting domes have been recently extended to several other systems, e.g., the Pu-based "115" compounds[84] and the high-T_c cuprates.[85,86] For example, $PuCoGa_5$ undergoes a superconducting transition at ~ 18.5 K,[87] one order of magnitude higher than the CeMIn$_5$ family. This compound shows no magnetic order,[88] being different from its sister compound $PuCoIn_5$ where superconductivity and magnetism are found to coexist.[84] On the other hand, it was shown that $PuCoGa_5$ is an intermediate valence compound.[89,90] Recent measurements of the elastic moduli demonstrate that valence fluctuations, as reflected by elastic softening, disappear as the temperature reaches T_c, indicating a close relationship between the formation of superconductivity and the avoidance of a valence transition.[91]

4. Quantum phase transitions

As described above, in heavy fermion compounds one can tune the ground state from magnetically ordered states (both AFM and FM) to a paramagnetic state by applying non-thermal parameters such as pressure, magnetic field, and chemical substitutions. Proper characterization of the quantum critical points and their related critical behaviors are currently an important but open problem in condensed matter physics. Elucidations of this problem may also aid in understanding the puzzles of unconventional superconductivity in heavy fermion compounds, high-T_c cuprates and other materials. Recently, two types of quantum critical points, the SDW-type QCP[52–54] and the local QCP,[50,51] have been studied intensively. Here the crucial point distinguishing these two scenarios is whether the degrees of electron freedom are involved at the QCP. The SDW-type QCP resembles a classical phase transition, where only fluctuations of the order parameter (e.g., magnetization for magnetic order) are involved and the Fermi surface changes smoothly across the QCP. On the other hand, the critical fermionic and bosonic degrees of freedom are involved at a local QCP, where a sharp change of the Fermi volume is expected as a result of a Kondo breakdown.

There is evidence that different tuning parameters may lead to different types of QCP. For example, the scenario of local quantum criticality has been discussed in $YbRh_2Si_2$ under a magnetic field[92] and $CeCu_{6-x}Au_x$ upon varying the doping,[93] although this is still under debate. On the other hand, evidence of Kondo destruction was found inside the antiferromagnetic region of Co-doped $YbRh_2Si_2$[94] as well as in magnetic-field tuned $CeCu_{6-x}Au_x$[95] and $Ce_3Pd_{20}Si_6$.[96] $CeCu_2Si_2$ is believed to be a 3D SDW-type QCP.[75]

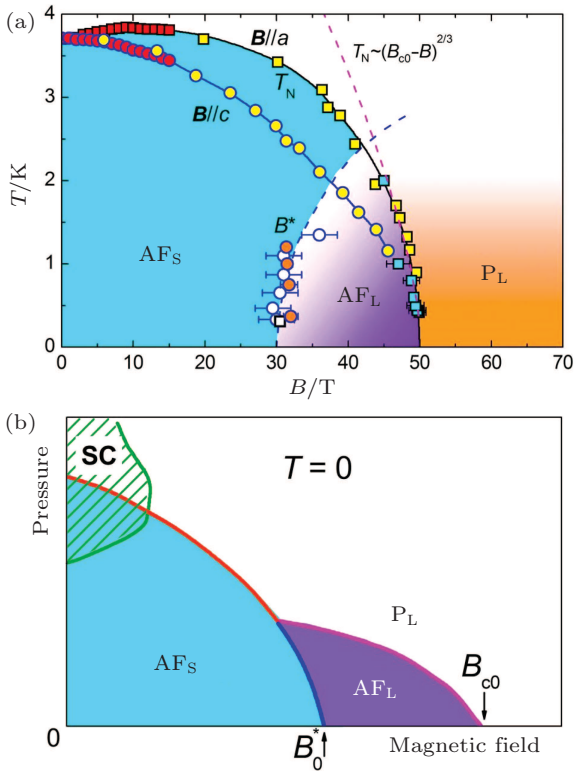


Fig. 10. (color online) (a) Experimental magnetic field–temperature phase diagram of $CeRhIn_5$ at ambient pressure. (b) A proposed schematic phase diagram for $CeRhIn_5$ at 0 K (adapted from Ref. [97]).

Recently, we demonstrated that $CeRhIn_5$ may serve as a model example to study multiple quantum phase transitions and their universal classification.[97] As mentioned earlier, there exists a pressure-induced antiferromagnetic QCP at around 2.3 GPa,[45] where a dramatic change of Fermi surface is observed,[49] supporting the scenario of local QCP in pressurized $CeRhIn_5$. Under a magnetic field, the antiferromagnetic transition of $CeRhIn_5$ is also suppressed and the large critical field allows us to study the field evolution of Fermi sur-

face using quantum oscillations. Figure 10(a) shows the magnetic field-temperature phase diagram of $CeRhIn_5$.[97] When a magnetic field is applied along the c direction, T_N is eventually suppressed and vanishes at $B_{c0} \approx 50$ T. Upon approaching the QCP, T_N follows $T_N \sim (B_{c0} - B)^{2/3}$, which indicates a 3D SDW-type QCP and is also consistent with the nearly isotropic critical field.[98] Furthermore, we observed a sharp change of the Fermi surface near $B^* \simeq 30$ T, well inside the antiferromagnetic phase, which is manifested in an abrupt change of the Hall coefficient and the sudden appearance of higher frequencies in dHvA measurements. The feature at B^* was further confirmed by recent transport measurements using single crystal microstructures fabricated using a focused ion beam.[99] Our analysis suggests that the Fermi surface reconstruction at B^* can be attributed to the localized-itinerant transition of Ce 4f electrons in $CeRhIn_5$, as a result of the Kondo effect.[97] Further studies are desirable in order to elucidate the nature of the Fermi surface reconstruction at B^*.

These results suggest that multiple quantum critical points may exist in $CeRhIn_5$ when tuned by different parameters and the change of the Fermi surface may serve as a criterion to classify the different scenarios.[97] It is important to further investigate the behaviors under both high pressure and high magnetic field which will be useful to establish the global phase diagram shown in Fig. 10(b). Our studies also provide a new perspective on heavy fermions and can be extended to other compounds with localized f electrons.

5. Summary and prospects

Physical pressure has proven to be a clean and powerful tool for tuning the electronic states of heavy fermion systems, which provides us with a great opportunity to study the intricate relationships between different ground states and to search for emergent quantum states or phenomena. In particular, exotic superconductivity emerges when heavy fermion systems are pressurized in proximity to various electronic instabilities, including antiferromagnetism, ferromagnetism and valence transitions. The insights gained from studying superconductivity in heavy fermion systems may play an important role in unveiling the mysterious superconducting mechanism in other unconventional superconductors such as cuprate, iron pnictides, and organic superconductors. Furthermore, heavy fermion compounds are also a prototype system for studying the physics of quantum criticality, a frontier problem in condensed matter physics. Advanced experimental methods, such as field-angle dependent heat capacity and point-contact spectroscopy under pressure, will be highly useful in characterizing their novel electronic states in a high-pressure environment.

References

[1] Kondo J 1964 *Prog. Theor. Phys.* **32** 37
[2] Stewart G R 1984 *Rev. Mod. Phys.* **56** 755
[3] Ruderman M A and Kittel C 1954 *Phys. Rev.* **96** 99
[4] Kasuya T 1956 *Prog. Theor. Phys.* **16** 45
[5] Yosida K 1957 *Phys. Rev.* **106** 893
[6] Doniach S 1977 *Physica B* **91** 231
[7] Steglich F, Aarts J, Bredl C D, Lieke, Meschede D, Franz W and Sch äfer H 1979 *Phys. Rev. Lett.* **43** 1892
[8] Sullivan P F and Seidel G 1968 *Phys. Rev.* **173** 679
[9] Wilhelm H 2003 *Adv. Solid State Phys.* **43** 889
[10] Vekhter I, Hirschfeld P J, Carbotte J P and Nicol E J 1999 *Phys. Rev. B* **59** R9023
[11] Matsuda Y, Izawa K and Vekhter I 2006 *J. Phys.: Condens. Matter* **18** R705
[12] An K, Sakakibara T, Settai R, Ōnuki Y, Hiragi M, Ichioka M and Machida K 2010 *Phys. Rev. Lett.* **104** 037002
[13] Izawa K, Yamaguchi H, Matsuda Y, Shishido H, Settai R and Ōnuki Y 2001 *Phys. Rev. Lett.* **87** 057002
[14] Park T and Thompson J D 2009 *New J. Phys.* **11** 055062
[15] Kasahara Y, Iwasawa T, Shimizu Y, Shishido H, Shibauchi T, Vekhter I and Matsuda Y 2008 *Phys. Rev. Lett.* **100** 207003
[16] Kambe S, Sakai H, Tokunaga Y and Walstedt R E 2010 *Phys. Rev. B* **82** 144503
[17] Kawasaki S, Zheng G Q, Kan H, Kitaoka Y, Shishido H and Ōnuki Y 2005 *Phys. Rev. Lett.* **94** 037007
[18] Yashima M, Tagami N, Taniguchi S, Unemori T, Uematsu K, Mukuda H, Kitaoka Y, Ōta Y, Honda F, Settai R and Ōnuki Y 2012 *Phys. Rev. Lett.* **109** 117001
[19] Pagliuso P G, Petrovic C, Movshovich R, Hall D, Hundley M F, Sarrao J L, Thompson J D and Fisk Z 2001 *Phys. Rev. B* **64** 100503
[20] Nicklas M, Sidorov V A, Borges H A, Pagliuso P G, Sarrao J L and Thompson J D 2004 *Phys. Rev. B* **70** 020505
[21] Lu X, Lee H, Park T, Ronning F, Bauer E D and Thompson J D 2012 *Phys. Rev. Lett.* **108** 027001
[22] Vekhter I and Vorontsov A 2008 *Physica B* **403** 958
[23] Daghero D and Gonnelli R S 2010 *Supercond. Sci. Technol.* **23** 043001
[24] Andreev A F 1964 *Sov. Phys. JETP* **19** 1228
[25] Blonder G E, Tinkham M and Klapwijk T M 1982 *Phys. Rev. B* **25** 4515
[26] Naidyuk Y G and Yanson I K 2005 *Point-Contact Spectroscopy* (New York: Springer-Verlag Inc.)
[27] Park W K, Sarrao J L, Thompson J D and Greene L H 2008 *Phys. Rev. Lett.* **100** 177001
[28] Park W K, Tobash P H, Ronning F, Bauer E D, Sarrao J L, Thompson J D and Greene L H 2012 *Phys. Rev. Lett.* **108** 246403
[29] Yang Y 2009 *Phy. Rev. B* **79** 241107
[30] Fogelström M, Graf M J, Sidorov V A, Lu X, Bauer E D and Thompson J D 2014 *Phys. Rev. B* **90** 104512
[31] Palstra T T M, Menovsky A A, Berg J, Dirkmaat A J, Kes P H, Nieuwenhuys G J and Mydosh J A 1985 *Phys. Rev. Lett.* **55** 2727
[32] Mydosh J A and Oppeneer P M 2011 *Rev. Mod. Phys.* **83** 1301
[33] Amitsuka H, Matsuda K, Kawasaki I, Tenya K, Yokoyama M, Sekine C, Tateiwa N, Kbayashi T C, Kawarazaki S and Yoshizawa H 2007 *J. Magn. Magn. Mater.* **310** 214
[34] Lu X, Ronning F, Tobash P H, Gofryk K, Bauer E D and Thompson J D 2012 *Phys. Rev. B* **85** 020402(R)
[35] Mathur N D, Grosche F M, Julian S R, Walker I R, Freye D M, Haselwimmer R K W and Lonzarich G G 1998 *Nature* **394** 39
[36] Steglich F, Buschinger B, Gegenwart P, Lohmann M, Helfrich R, Langhammer C, Hellmann P, Donnevert L, Thomas S, Link A, Geibel C, Lang M, Sparn G and Assmus W 1996 *J. Phys.: Condens. Matter* **8** 9909
[37] Petrovic C, Pagliuso P G, Hundley M F, Movshovich R, Sarrao J L, Thompson J D, Fisk Z and Monthoux P 2001 *J. Phys.: Condens. Matter* **13** L337
[38] Hegger H, Petrovic C, Moshopoulou E G, Hundley M F, Sarrao J L, Fisk Z and Thompson J D 2000 *Phys. Rev. Lett.* **84** 4986
[39] Petrovic C, Movshovich R, Jaime M, Pagliuso P G, Hundley M F, Sarrao J L, Fisk Z and Thompson J D 2001 *Europhys. Lett.* **53** 354
[40] Kimura N, Ito K, Saitoh K, Umeda Y, Aoki H and Terashima T 2005 *Phys. Rev. Lett.* **95** 247004
[41] Sugitani I, Okuda Y, Shishido H, Yamada T, Thamizhavel A, Yamamoto E, Matsuda T D, Haga Y, Takeuchi T, Settai R and Ōnuki Y 2006 *J. Phys. Soc. Jpn.* **75** 043703

[42] Nicklas M, Borth R, Lengyel E, Pagliuso P G, Sarrao J L, Sidorov V A, Sparn G, Steglich F and Thompson J D 2001 *J. Phys.: Condens. Matter* **13** L905
[43] Sidorov V A, Nicklas M, Pagliuso P G, Sarrao J L, Bang Y, Balatsky A V and Thompson J D 2002 *Phys. Rev. Lett.* **89** 157004
[44] Kohori Y, Yamato Y, Iwamoto Y, Kohara T, Bauer E D, Maple M B and Sarrao J L 2001 *Phys. Rev. B* **64** 134526
[45] Park T, Ronning F, Yuan H Q, Salamon M B, Movshovich R, Sarrao J L and Thompson J D 2006 *Nature* **440** 65
[46] Knebel G, Aoki D, Braithwaite D, Salce B and Flouquet J 2006 *Phys. Rev. B* **74** 020501(R)
[47] Aso N, Ishii K, Yoshizawa H, Fujiwara T, Uwatoko Y, Chen G F, Sato N K and Miyake K 2009 *J. Phys. Soc. Jpn.* **78** 073703
[48] Park T, Sidorov V A, Ronning F, Zhu J X, Tokiwa Y, Lee H, Bauer E D, Movshovich R, Sarrao J L and Thompson J D 2008 *Nature* **456** 366
[49] Shishido H, Settai R, Harima H and Ōnuki Y 2005 *J. Phys. Soc. Jpn.* **74** 1103
[50] Si Q, Rabello S, Ingersent K and Smith J L 2001 *Nature* **413** 804
[51] Coleman P and Schofield A J 2005 *Nature* **433** 226
[52] Hertz J A 1976 *Phys. Rev. B* **14** 1165
[53] Millis A J 1993 *Phys. Rev. B* **48** 7183
[54] Moriya T and Takimoto T 1995 *J. Phys. Soc. Jpn.* **64** 960
[55] Sidorov V A, Lu X, Park T, Lee H, Tobash P H, Baumbach R E, Ronning F, Bauer E D and Thompson J D 2013 *Phys. Rev. B* **88** 020503
[56] Bianchi A, Movshovich R, Jaime M, Thompson J D, Pagliuso P G and Sarrao J L 2001 *Phys. Rev. B* **64** 220504
[57] Muramatsu T, Kobayashi T C, Shimizu K, Amaya K, Aoki D, Haga Y and Ōnuki Y 2003 *Physica C* **388** 539
[58] Pham L D, Park T, Maquilon S, Thompson J D and Fisk Z 2006 *Phys. Rev. Lett.* **97** 056404
[59] Chen Y, Jiang W B, Guo C Y, Ronning F, Bauer E D, Park T, Yuan H Q, Fisk Z, Thompson J D and Lu X 2015 *Phys. Rev. Lett.* **114** 146403
[60] Shang T, Baumbach R E, Gofryk K, Ronning F, Weng Z F, Zhang J L, Lu X, Bauer E D, Thompson J D and Yuan H Q 2014 *Phys. Rev. B* **89** 041101
[61] Levy F, Sheikin I, Grenier B and Huxley A D 2005 *Science* **309** 1343
[62] Huy N T, Gasparini A, Nijs D E, Huang Y, Klaasse J C P, Gortenmulder T, Visser A, Hamann A, Görlach T and Löhneysen H V 2007 *Phys. Rev. Lett.* **99** 067006
[63] Saxena S S, Agarwal1 P, Ahilan K, Grosche F M, Haselwimmer R KW, Steiner M J, Pugh E, Walker I R, Julian S R, Monthoux P, Lonzarich G G, Huxley A, Sheikin I, Braithwaite D and Flouquet J 2000 *Nature* **406** 587
[64] Kobayashi T C, Hori A, Fukushima S, Hidaka H, Kotegawa H, Akazawa T, Takeda K, Ohishi Y and Yamamoto E 2007 *J. Phys. Soc. Jpn.* **76** 051007
[65] Ōnuki Y, Ukon I, Yun S W, Umehara I, Satoh K, Fukuhara T, Sato H, Takayanagi S, Shikama M and Ochiai A 1992 *J. Phys. Soc. Jpn.* **61** 293
[66] Terashima T, Matsumoto T, Terakura C, Uji S, Kimura N, Endo M, Komatsubara T and Aoki H 2001 *Phys. Rev. Lett.* **87** 166401
[67] Oomi G, Kagayama K, Nishimura K, Yun S W and Ōnuki Y 1995 *Physica B* **206** 515
[68] Huxley A D, Sheikin I, Ressouche E, Kernavanois N, Braithwaite D, Calemczuk R and Flouquet J 2001 *Phys. Rev. B* **63** 144519
[69] Tran V H, Paschen S, Troc R, Baenitz M and Steglich F 2004 *Phys. Rev. B* **69** 195314
[70] Misiorek H, Mucha J, Troc R and Coqblin B 2005 *J. Phys.: Condens. Matter* **17** 679
[71] Ito T, Kumigashira H, Souma S, Takahashi T, Haga Y and Ōnuki Y 2002 *J. Phys. Soc. Jpn.* **71** 265
[72] Pfleiderer C and Huxley A D 2002 *Phys. Rev. Lett.* **89** 147005
[73] Watanabe S and Miyake K 2002 *J. Phys. Soc. Jpn.* **71** 2489
[74] Shick A B, Janiš V, Drchal V and Pickett W E 2004 *Phys. Rev. B* **70** 134506
[75] Stockert O, Faulhaber E, Zwicknagl G, Stüber N, Jeevan H S, Deppe M, Borth R, Küchler R, Loewenhaupt M, Geibel C and Steglich F 2004 *Phys. Rev. Lett.* **92** 136401
[76] Thomas F, Ayache C, Fomine I A, Thomasson J and Geibel C 1996 *J. Phys.: Condens. Matter* **8** L51
[77] Yuan H Q, Grosche F M, Deppe M, Geibel C, Sparn G and Steglich F 2003 *Science* **302** 2104
[78] Yuan H Q, Grosche F M, Deppe M, Geibel C, Sparn G and Steglich F 2006 *Phys. Rev. Lett.* **96** 047008
[79] Yuan H Q, Grosche F M, Deppe M, Geibel C, Sparn G and Steglich F 2004 *New J. Phys.* **11** 055062
[80] Kittaka S, Aoki Y, Shimura Y, Sakakibara T, Seiro S, Geibel C, Steglich F, Ikeda H and Machida K 2014 *Phys. Rev. Lett.* **112** 067002
[81] Lengyel E, Nicklas M, Jeevan H S, Sparn G, Geibel C, Steglich F, Yoshioka Y and Miyake K 2009 *Phys. Rev. B* **80** 140513
[82] Holmes A T, Jaccard D and Miyake K 2004 *Phys. Rev. B* **69** 024508
[83] Onishi Y and Miyake K 2000 *J. Phys. Soc. Jpn.* **69** 3955
[84] Bauer E D, Altarawneh M M, Tobash P H, Gofryk K, Ayala-Valenzuela O E, Mitchell J N, McDonald R D, Mielke C H, Ronning F and Griveau J C 2012 *J. Phys.: Condens. Matter* **24** 052206
[85] Tranquada J M, Sternlieb B J, Axe J D, Nakamura Y and Uchida S 1995 *Nature* **375** 561
[86] Wu T, Mayaffre H, Krämer S, Horvatić M, Berthier C, Hardy W N, Liang R X, Bonn D A and Julien M H 2011 *Nature* **477** 191
[87] Sarrao J L, Morales L A, Thompson J D, Scott B L, Stewart G R, Wastin F, Rebizant J, Boulet P, Colineau E and Lande G H 2002 *Nature* **420** 297
[88] Hiess A, Stunault A, Colineau E, Rebizant J, Wastin F, Caciuffo R and Lander G H 2008 *Phys. Rev. Lett.* **100** 076403
[89] Joyce J J, Wills J M, Durakiewicz T, Butterfield M T, Guziewicz E, Sarrao J L, Morales L A, Arko A J and Eriksson O 2003 *Phys. Rev. Lett.* **91** 176401
[90] Pezzoli M E, Haule K and Kotliar G 2011 *Phys. Rev. Lett.* **106** 016403
[91] Ramshaw B J, Shekhter A, McDonald R D, Betts J B, Mitchell J N, Tobash P H, Mielke C H, Bauer E D and Migliori A 2015 *Proc. Natl. Acad. Sci.* **112** 3285
[92] Paschen S, L, hmann T, Wirth S, Gegenwart P, Trovarelli O, Geibel C, Steglich F, Coleman P and Si Q 2004 *Nature* **432** 881
[93] Schröder A, Aeppli G, Coldea R, Adams M, Stockert O, Löhneysen H V, Bucher E, Ramazashvili R and Coleman P 2000 *Nature* **407** 351
[94] Friedemann S, Westerkamp T, Brando M, Oeschler N, Wirth S, Gegenwart P, Krellner C, Geibel C and Steglich F 2009 *Nat. Phys.* **5** 465
[95] Stockert O, Enderle M and Löhneysen H V 2007 *Phys. Rev. Lett.* **99** 237203
[96] Custers J, Lorenzer K A, Müller M, Prokofiev A, Sidorenko A, Winkler H, Strydom A M, Shimura Y, Sakakibara T, Yu R, Si Q and Paschen S 2012 *Nat. Mater.* **11** 189
[97] Jiao L, Chen Y, Kohama Y, Graf D, Bauer E D, Singleton J, Zhu J X, Weng Z F, Pang G M, Shang T, Zhang J L, Lee H O, Park T, Jaime M, Thompson J D, Steglich F, Si Q and Yuan H Q 2015 *Proc. Natl. Acad. Sci.* **112** 673
[98] Millis A J 1993 *Phys. Rev. B* **48** 7183
[99] Moll P J W, Zeng B, Balicas L, Galeski S, Balakirev F F, Bauer E D and Ronning F 2015 *Nat. Commun.* **6** 6663